

Frequency stabilization of an extended cavity semiconductor diode laser for chirp cooling

J. Morzinski

Research Laboratory of Electronics, Massachusetts Institute of Technology, Cambridge, Massachusetts 02139

P. S. Bhatia and M. S. Shahriar^{a)}

Research Laboratory of Electronics, Massachusetts Institute of Technology, Cambridge, Massachusetts 02139
and Department of Electrical and Computer Engineering, Northwestern University, Evanston, Illinois 60208

(Received 2 November 2001; accepted for publication 30 June 2002)

We present a technique to stabilize in an atomic transition the chirping frequency of a narrow-band semiconductor diode laser. The technique is demonstrated to chirp-cool ^{85}Rb atoms used for loading a magneto-optical trap. The stabilization process eliminates long-term fluctuations and drifts in the number of atoms caught in the trap. This is a simple, easy-to-implement, and robust method for wide range of laser cooling experiments employing frequency chirping. © 2002 American Institute of Physics. [DOI: 10.1063/1.1502443]

I. INTRODUCTION

Cooling and trapping of atoms¹ is of considerable current interest. In laser cooling experiments atoms scatter resonant photons from a laser beam directed against the velocity of the atomic beam. The transfer of photon momentum to the atom eventually brings the atom to rest. The primary experimental difficulty in such atom-slowng techniques is the varying Doppler shift experienced by the atom as it slows down. The change in the Doppler shift takes the atom out of resonance with the laser field. Therefore, to keep the atom on resonance with the applied field as it slows down, either the atomic or the laser frequency needs to be smoothly and accurately varied. The technique based on varying the atomic frequency is called Zeeman cooling,² while the corresponding technique based on varying the laser frequency is called chirp cooling.^{3–6} In both techniques the laser is detuned to be below the zero-velocity resonance frequency of the moving atom. The detuning is chosen to be such that the atoms moving with the most probable velocity, u , in the Maxwell–Boltzmann distribution are on resonance with the laser at the start of the slowing process. As these atoms slow down, the Doppler shifts decrease, and therefore, to keep the atom in resonance, the laser frequency must increase. In the case of chirp cooling, this is achieved by sweeping the laser frequency as a function of time at a rate equal to the ratio of the Doppler shift at the most probable velocity of the atoms to the total time needed for stopping the atoms. For this process, diode lasers are often used, partly because of their compactness and low cost,^{7–9} and because chirp is easier to achieve with diode lasers. Diode lasers, however, suffer from the frequency drift caused by changes in the junction temperature, by current noise, and by the perturbation of the external cavity length used for narrowing the laser spectrum. The irregular frequency results in inefficient cooling, as well as changes in the final velocity profile of the atomic beam.

This problem can be overcome by using, for example, an acousto-optic modulator (AOM). Briefly, the diode laser frequency is shifted by the AOM, and then locked to an atomic transition using standard methods.^{10–13} The AOM driving frequency is then scanned in order to produce the required chirping. One drawback of this approach is that the direction of the output of an AOM is correlated with the driving frequency, so that the scan is accompanied by undesired angular variations. One can overcome this problem by using a compensating, scanning mirror. However, in order for this process to work well, the scan range should be a small fraction of the base frequency. Given that the scan range is typically a few hundred MHz, this implies that the AOM to be used should have a base frequency in the GHz range. An AOM at such a high frequency is generally expensive, and not very efficient. As such, only a small fraction of the total diode laser power is available for chirp cooling. In this article, we demonstrate an alternative method that does not require an AOM, and makes most of the diode laser power available for

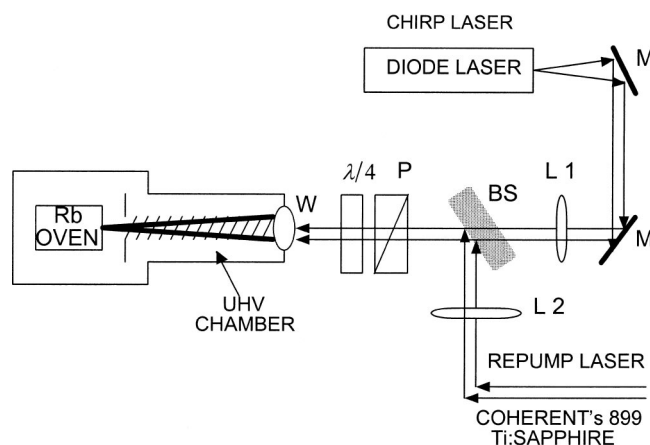


FIG. 1. Experimental apparatus employed for the chirp cooling. UHV: ultrahigh vacuum; $\lambda/4$: quarter-wave plate; P: polarizer; BS: beam splitter; L1, L2 lenses; and M: turning mirror.

^{a)}Electronic mail: shahriar@ece.nwu.edu

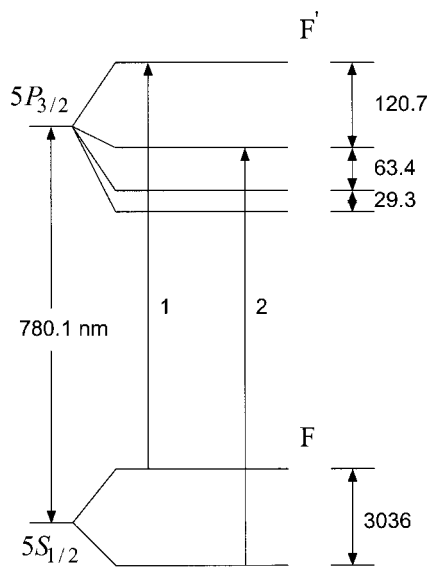


FIG. 2. Energy-level splitting of ^{85}Rb . Chirp and repump lasers are tuned to the transitions with labels 1 and 2, respectively.

cooling. It is simple, robust, and requires only inexpensive electronics.

II. EXPERIMENTAL CONFIGURATION

In our experimental setup, shown in Fig. 1, the beam consists of rubidium atoms, which effuse from a small hole about $100\ \mu\text{m}$ in diameter in an oven operating at $\approx 250\ ^\circ\text{C}$. The atomic beam is collimated by a second aperture with a diameter of about $300\ \mu\text{m}$, and directed into a vacuum chamber evacuated to about 10^{-10} Torr. The most probable velocity, $u[\approx \sqrt{(2K_B T/M)}$, where K_B is the Boltzmann constant, T is the oven temperature in kelvin, and M is the atomic mass] of the ^{85}Rb atoms in the atomic beam is $\approx 320\ \text{m/s}$, which corresponds to the Doppler shift of about 420 MHz. To chirp cool the atoms in this atomic beam we use a commercially adopted version (Tui Optics: DL 100) of the extended-cavity diode laser described earlier by Hansch and co-workers.⁸ This system uses a solitary laser diode (manufactured by Hitachi, Part No. HL-7857 G), which operates near 780 nm. When free running, this laser operates in multimode with a broad spectrum. In this laser system, external

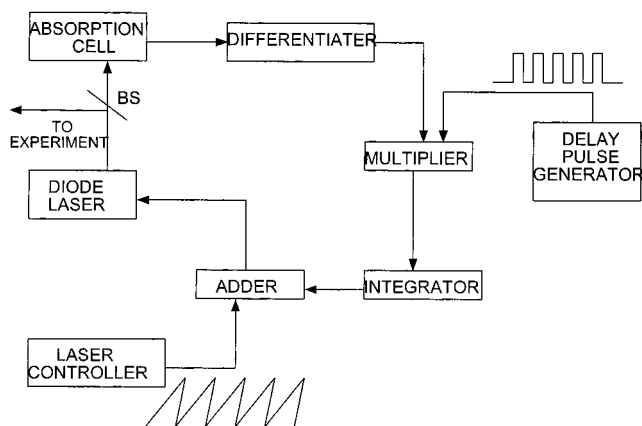


FIG. 3. Block diagram of the electronic circuit used to stabilize the chirp laser.

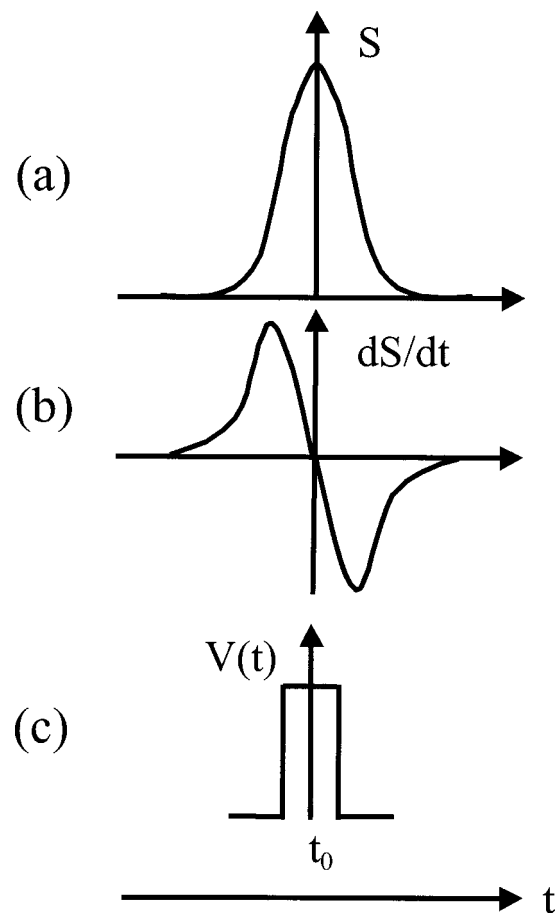


FIG. 4. (a) Absorption signal, (b) differentiated signal, and (c) pulse from pulse generator; t_0 is the zero-crossing point of the differentiated signal.

feedback to the laser diode provided by a grating in the Littrow configuration forces the laser to operate in single mode with a linewidth of about 1 MHz.⁹ The course tuning of the laser output wavelength is achieved by changing the junction temperature and the injection current of the laser diode, while the fine tuning is achieved by changing the tilt angle of the diffraction grating with a piezoactuator. This diode laser beam is overlapped with a second repump laser beam. The two superimposed beams are circularly polarized and focused inside the vacuum chamber, where they overlap and propagate counter to the atomic beam. Inside the vacuum chamber there is about 10 mW of diode laser power with a beam diameter of 5 mm, and about 75 mW of repump laser power with a beam diameter of 1 cm, with different divergences. These beams are combined on a polarizing beam splitter, and focused with a long focal length ($f=1\ \text{m}$) lens onto the first ($100\ \mu\text{m}$ diam) hole at the origin of the atomic beam. The divergences of both beams are adjusted outside the vacuum chamber in order to ensure that each beam has an estimated beam diameter of about $100\ \mu\text{m}$ at the beam origin. As shown in Fig. 2, the diode laser is tuned to the $5S_{1/2}(F=3) \rightarrow 5P_{3/2}(F'=4)$ transition of the ^{85}Rb atom. The diode laser beam decelerates the ^{85}Rb atoms, which are finally brought to rest. The total stopping distance in our experiment is about 1 m. The function of the repump beam is to prevent the optical pumping of the atoms into the lower hyperfine level $5S_{1/2}(F=2)$ of the ground state (Fig. 2).^{4,14}

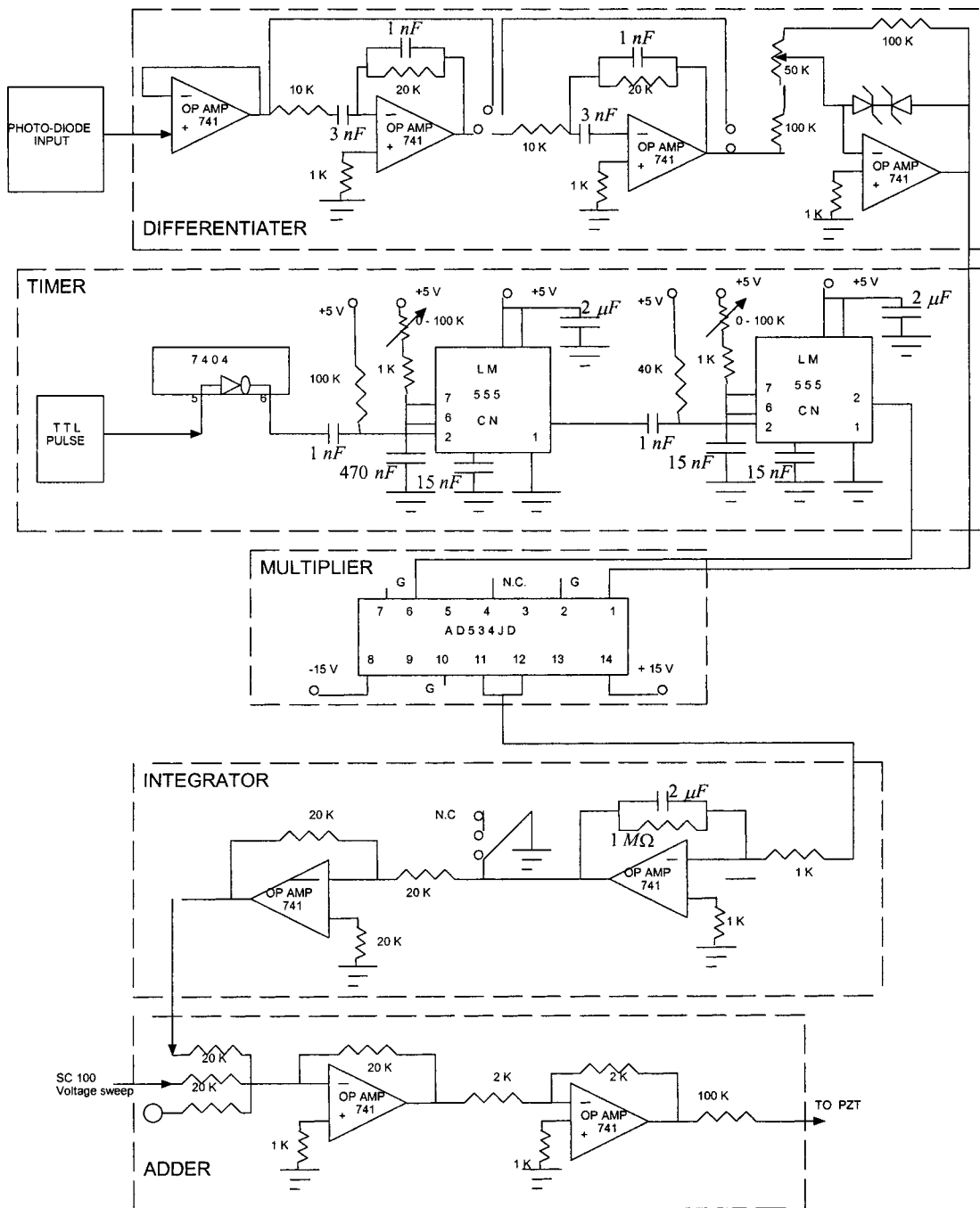


FIG. 5. Schematic of the electronic circuit.

The repump beam is generated from a Ti-sapphire laser, and is locked to the zero-velocity transition corresponding to $5S_{1/2}(F=2) \rightarrow 5P_{3/2}(F'=3)$, using a saturated absorption cell. The saturation intensity [defined as the intensity that produces a Rabi frequency equaling the population decay rate (~ 6 MHz) divided by $\sqrt{2}$] of this transition (averaged over the magnetic sublevel) is about 6 mW/cm^2 [as compared to 1.5 mW/cm^2 for the strongest, cycling transition: $(F=3, m_F=3) \rightarrow (F'=4, m_F=4)$.] With a beam of 75 mW focused to a $100 \mu\text{m}$ spot, the resulting intensity is about 10^6 mW/cm^2 , which corresponds to roughly 1.6×10^5 times the saturation intensity. Given that the Rabi frequency is proportional to the square root of the intensity, this produces a Rabi frequency of about 1.7 GHz , which is more

than adequate to power broaden the transition to cover effectively the Doppler shift of $\sim 420 \text{ MHz}$ of the most probable velocity. Of course, as the atom moves away from the starting point, the intensity becomes smaller (since the beam is no longer focused). This effect is largely compensated significantly by the fact that the atoms also slow down, thus reducing the Doppler shift. However, we have observed that increasing the repump power (up to 400 mW) increases the number of atoms trapped, indicated that the power used (75 mW) is suboptimal. Ideally, more efficient slowing would result if one were to scan the repump laser as well. Instead, whenever it is necessary to maximize the number of atoms trapped, we simply increase the repump power.

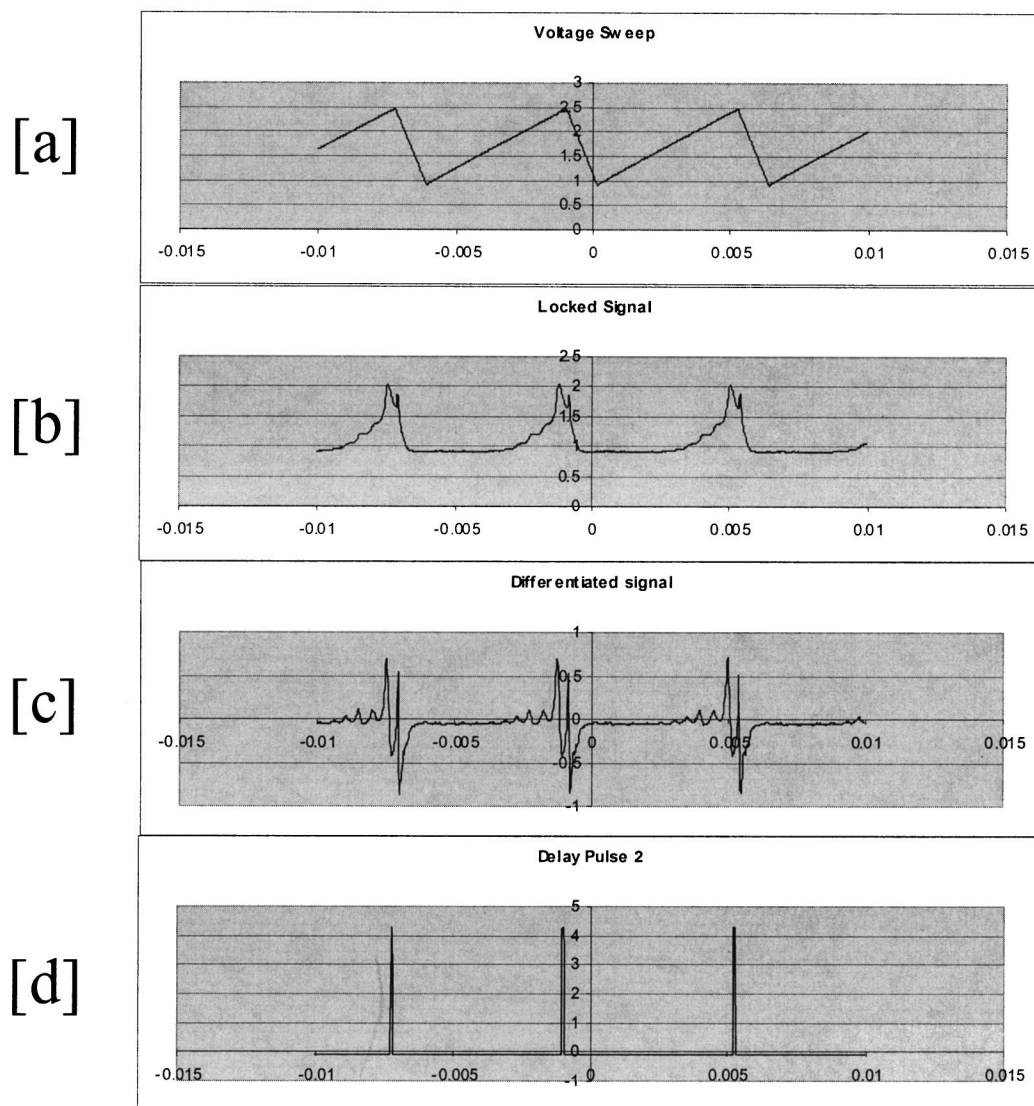


FIG. 6. (a) Voltage sweep, (b) absorption signal, (c) differentiated signal, and (d) pulse from pulse generator.

III. STABILIZATION MECHANISM

A block diagram of the locking circuit is shown in Fig. 3. The diode laser frequency is swept by a voltage ramp from the laser controller, which is also applied to the grating drive mechanism of the diode laser. The sweeps are very short (~ 6 ms), compared to the duration over which the drift becomes significant. Specifically, for slowing purposes, a drift of the order of the natural linewidth (~ 6 MHz) is considered significant. A drift of this amount takes about 3 s, which corresponds to a drift of about 12 kHz during the scan. As such, it is adequate to apply the feedback signal only after each sweep. The absorption spectrum was monitored with a photodiode through another vapor cell containing rubidium atoms, using the process of saturated absorption. This spectrum was recorded at room temperature at which the Doppler width (full width half maximum) is $2u \approx 600$ MHz. The signal from the photodiode is differentiated electronically. The differentiated signal is then multiplied by the output of the pulse generator, which generates transistor-transistor logic pulses with adjustable time delay. The product of the differentiated signal and the delay pulses is supplied to an integra-

tor. The integrated output is the feedback signal, which is added to the ramp voltage that drives the grating to sweep the laser frequency.

To lock the sweeping laser frequency, the time delay of the pulse from the pulse generator is adjusted so that the pulse coincides with the zero-crossing point of the differentiated signal (Fig. 4). Under this condition the error signal is zero. Any drift in the laser output frequency results in an offset between the pulse from the pulse generator and the zero-crossing point of the differentiated signal. This results in a nonzero value of the error signal, whose magnitude and sign are determined by that of the offset. Figure 5 shows the schematic of the actual circuit. The complete circuit consists of four essential parts viz. (1) differentiator, (2) timer, (3) integrator, and (4) adder.

Figure 6 shows a typical signal as experimentally observed through the absorption cell containing ^{85}Rb atoms. This signal was observed using the ramp voltage shown in Fig. 6(a). Figure 6(c) shows the output of the differentiator when the signal shown in Fig. 6(a) was supplied to its input. In Fig. 6 the peak position of the signal and the zero-crossing

point of the differentiated signal are coincident with the pulse from the pulse generator shown in Fig. 6(d). Some kinks in Figs. 6(b) and 6(c) are due to the presence of the neighboring hyperfine transitions shown in Fig. 2, which lies within the Doppler envelope and complicates the interpretation of the observed spectrums.

In our experiment, chirp-cooled atoms are loaded into the magneto-optical trap, where three pairs of counterpropagating laser beams subsequently trap them. With the feedback loop shown in Fig. 3 closed, we typically achieve a stable trap with approximately ten million atoms. As the feedback loop is opened, the trap gets weaker and finally disappears in a few minutes, illustrating the potential importance of using laser stabilization during chirp cooling. With the feedback loop closed, the trap intensity remains stable for about 3 h before it is necessary to reset the servo.

In conclusion, we have presented a technique and its implementation to stabilize the chirping frequency of a diode laser. The technique is simple and robust, requiring only simple electronics. *Furthermore, this technique allows stabilizing the chirp for several continuous hours.* This stabilization process eliminates long-term fluctuations and drifts in the number of atoms caught in a magneto-optic trap, for example.

ACKNOWLEDGMENTS

This work was supported by AFOSR Grant No. F49620-98-1-0313 and ARO Grant No. DAAG55-98-1-0375 and DAAD19-00-1-0177.

- ¹H. J. Metcalf and P. van der Straten, *Laser Cooling and Trapping* (Springer, Berlin, 1999).
- ²J. Prodan, A. Migdall, W. D. Phillips, I. So, H. Metcalf, and J. Dalibard, *Phys. Rev. Lett.* **54**, 992 (1985).
- ³W. Ertmer, R. Blatt, J. L. Hall, and M. Zhu, *Phys. Rev. Lett.* **54**, 996 (1985).
- ⁴R. N. Watts and C. E. Wieman, *Opt. Lett.* **11**, 291 (1986).
- ⁵C. C. Bradley, J. G. Story, J. J. Tollett, J. Chen, N. W. M. Ritchie, and R. G. Hulet, *Opt. Lett.* **17**, 349 (1992).
- ⁶V. I. Balykin, V. S. Letokhov, and V. I. Mushin, *JETP Lett.* **29**, 560 (1979).
- ⁷C. E. Wieman and L. Hollberg, *Rev. Sci. Instrum.* **62**, 1 (1991).
- ⁸L. Ricci, M. Weidemuller, T. Esslinger, A. Hemmerich, C. Zimmermann, V. Vuletic, W. Konig, and T. W. Hansch, *Opt. Commun.* **117**, 541 (1995).
- ⁹P. S. Bhatia, G. R. Welch, and M. O. Scully, *Opt. Commun.* **189**, 321 (2001).
- ¹⁰M. de Labachellerie and P. Cerez, *Proc. SPIE* **701**, 182 (1986).
- ¹¹T. P. Dinneen, C. D. Wallace, and P. L. Gould, *Opt. Commun.* **92**, 277 (1992).
- ¹²M. de Labachellerie, C. Latrasse, K. Diomande, P. Kemssu, and P. Cerez, *IEEE Trans. Instrum. Meas.* **40**, 185 (1991).
- ¹³Y. Millerioux, D. Touahi, L. Hilico, A. Clairon, R. Felder, F. Biraben, and B. de Beauvoir, *Opt. Commun.* **108**, 91 (1994).
- ¹⁴C. D. Wallace, Ph.D. thesis, University of Connecticut, 1994.